Off-Axis Fatigue Behavior of a Plain Weave Carbon/Epoxy Fabric Laminate at Room and High Temperatures and Its Mechanical Modeling

M. Kawai and T. Taniguchi

Division of Engineering Mechanics and Energy
Graduate School of Systems and Information Engineering
University of Tsukuba, Japan

Outline

1. Background
2. Objectives
3. Experimental results
4. Modeling and predictions
5. Summary

Woven Fabric Composites

Attractive Features (e.g. Kelly, 1989):

- Lower fabrication cost
- Better drapeability/shapeability
- Ease of handling
- Better damage tolerance, esp. against impact
- Improved intra- and inter-lamina strengths
  (Multidirectional reinforcement in a single layer)

Woven Carbon Fabric Composites

Suitability for Near Net Shape Manufacturing:

- Plates and shell structures
- Large-scale structures

(From J. Hinrichsen, Japan SAMPE, 2001)

Woven CFRP

Primary aerospace structures

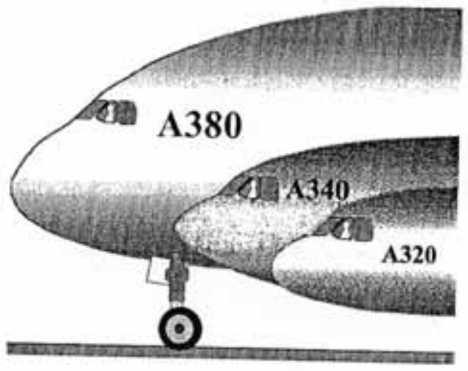

Fig. 2: Size Comparison

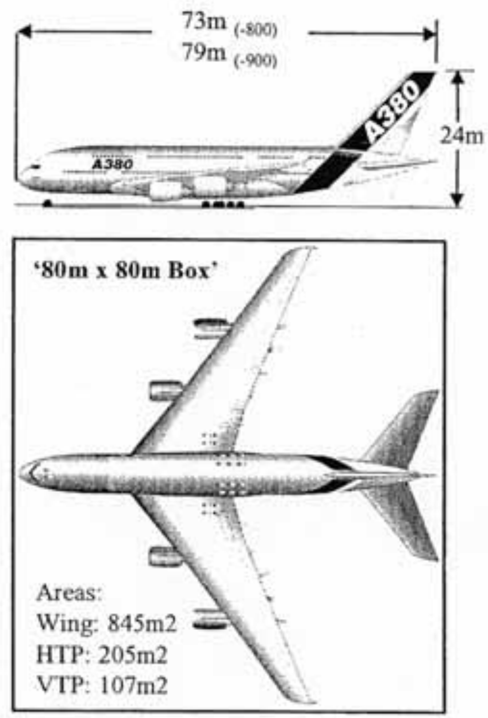

Fig. 1: A380 Outer Dimensions

Durability prediction

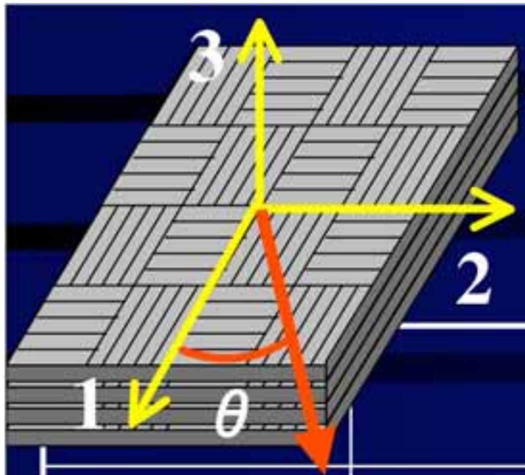

Fatigue of WFC

U: unnotched; **N**: notched; **P**: plain; **S**: satin; **K**: knitted;

	Woven GFRP	Woven CFRP
On-axis	Boller (1957) U+N+P Xiao-Bathias (1994) U+N+P Yamamoto-Hyakutake (1999) U+N+P Paepegem-Degrieck (2001) U+P **+ much more**	Shimokawa-Hamaguchi (1983) N+S Hamaguchi-Shimokawa (1987) N+S Schulte et al. (1987) U+S Miyano et al. (1994) U+S Kawai et al. (1996) U+N+P Khan et al. (2002) U+P
Off-axis	Owen-Bishop (1972,1973) U+N+P Owen-Griffiths (1978) U+N+P Wang et al. (1982) U+P Smith-Pascoe (1989) U+P Amijima et al. (1991) U+P Fujii et al. (1993-1996) U+N+P Hansen (1999) U+N+P Pandita-Verpoest (2001,2004) U+P+K	Very few !

Objectives

For a plain woven CFRP laminate,

1. Experimental

- Off-axis tensile behavior
- Off-axis fatigue behavior
- Temperature dependence

2. Theoretical

- Phenomenological modeling
- Predictions

Material System

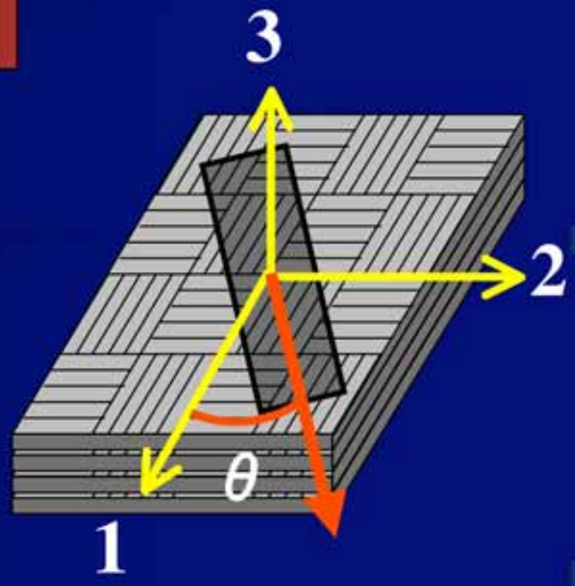

T300/Epoxy#2500
Plain woven roving cloth prepreg
(12-ply laminates)

Standard specimens:

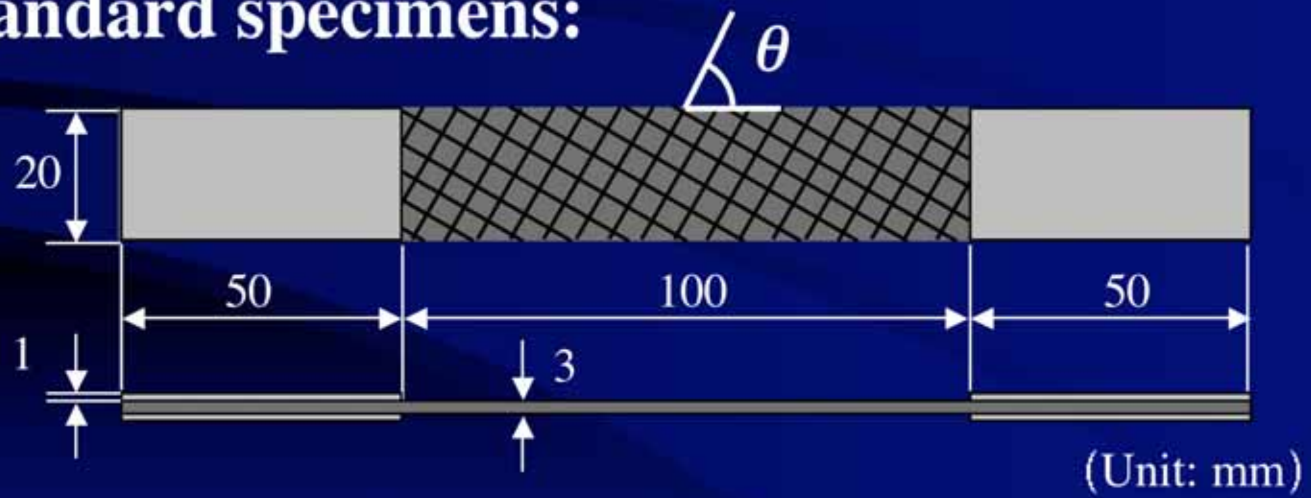

Off-axis fiber orientations: $\theta = 0, 15, 30, 45, 90^{\circ}$

Tension Test

Stroke control: 1.0 mm/min
Temperature: RT (~25°C) and 100°C

Fatigue Test

Load control :
Wave shape: Sinusoidal
Frequency: $f = 10$ Hz (+ 2 Hz)
Stress ratio: $R = \sigma_{min}/\sigma_{max} = 0.1$
Temperature: RT (~25°C) and 100°C

Off-Axis Stress-Strain Curves

$\theta = 0 \sim 90^\circ$; RT

$\theta = 0, 15, 45^\circ$; RT, 100°C

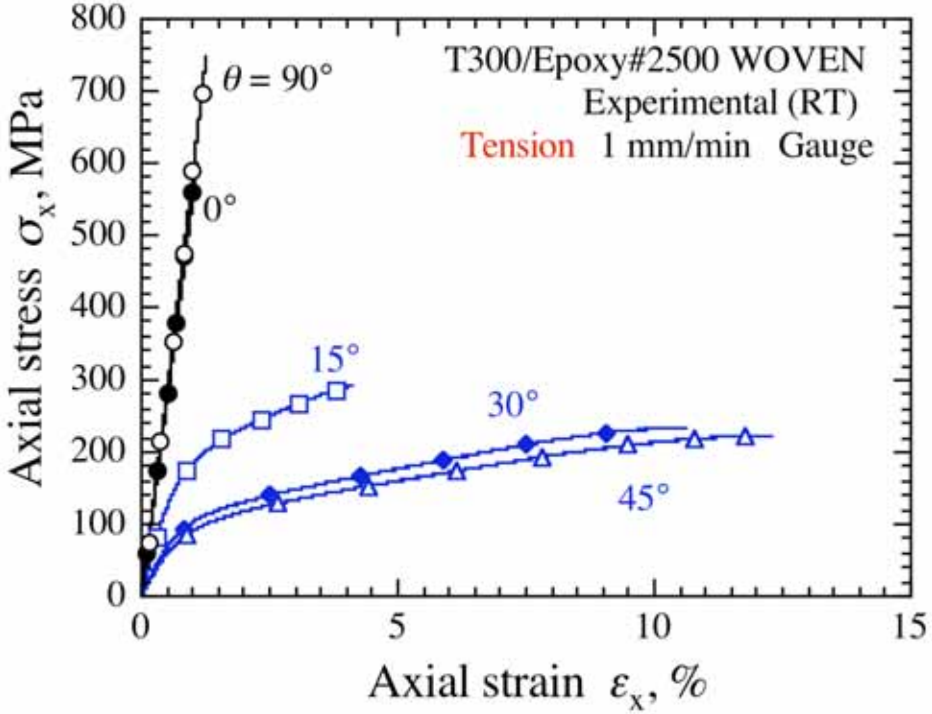

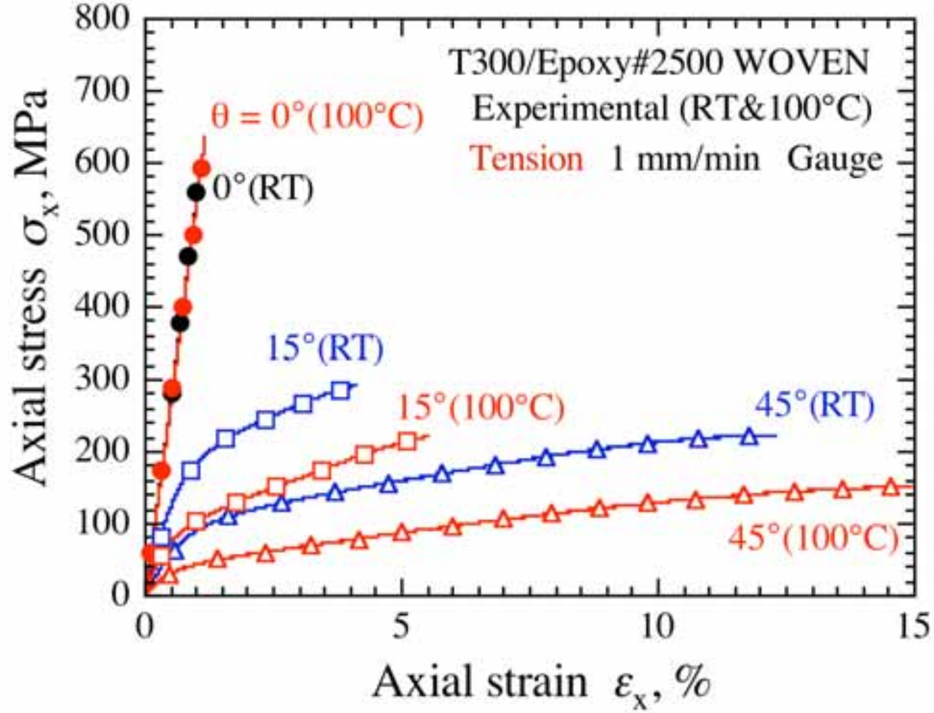

Fiber orientation dependence

Temperature dependence

Off-Axis Tensile Strength

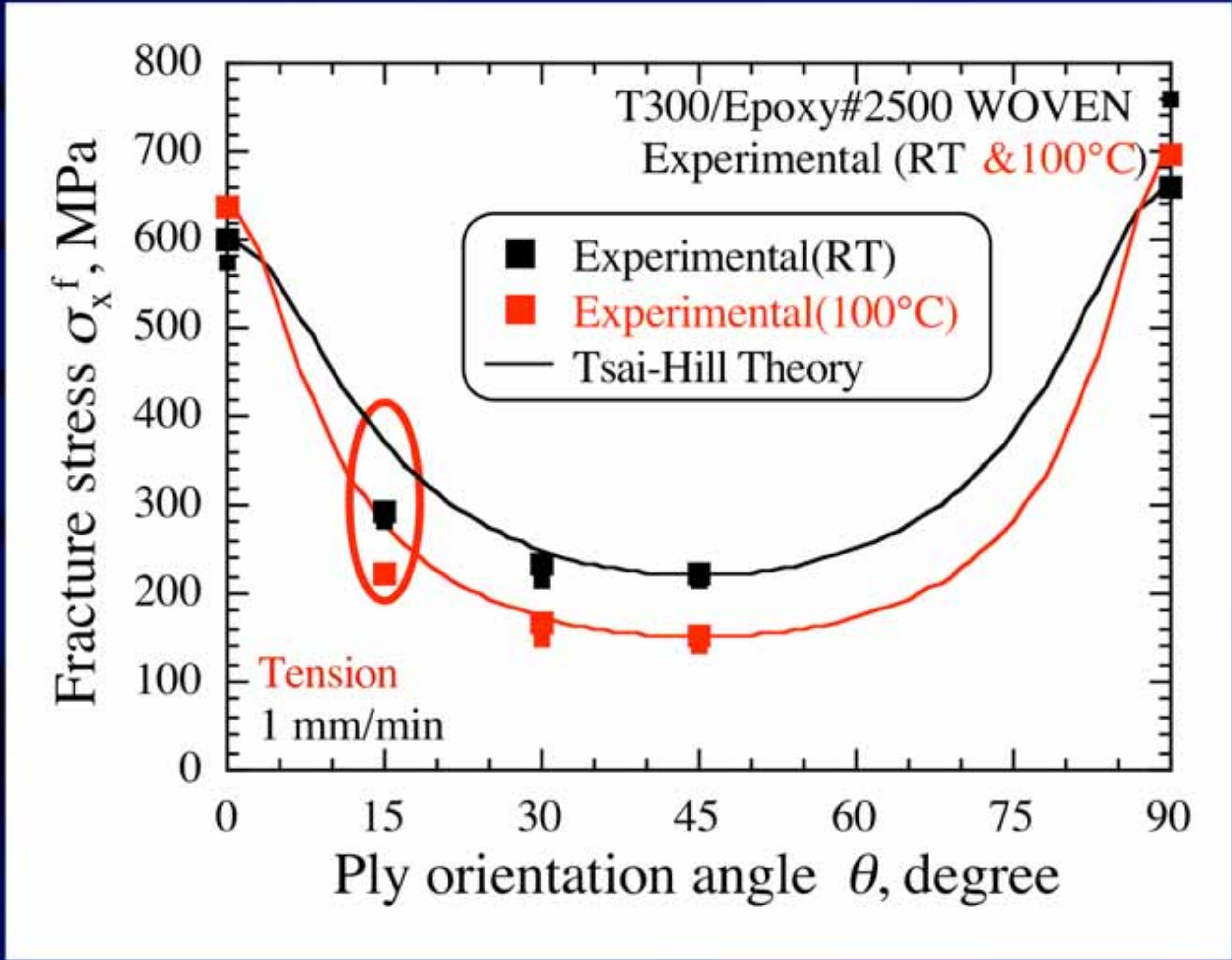

Off-Axis S-N Relationships

based on a maximum fatigue stress (σ_{max})

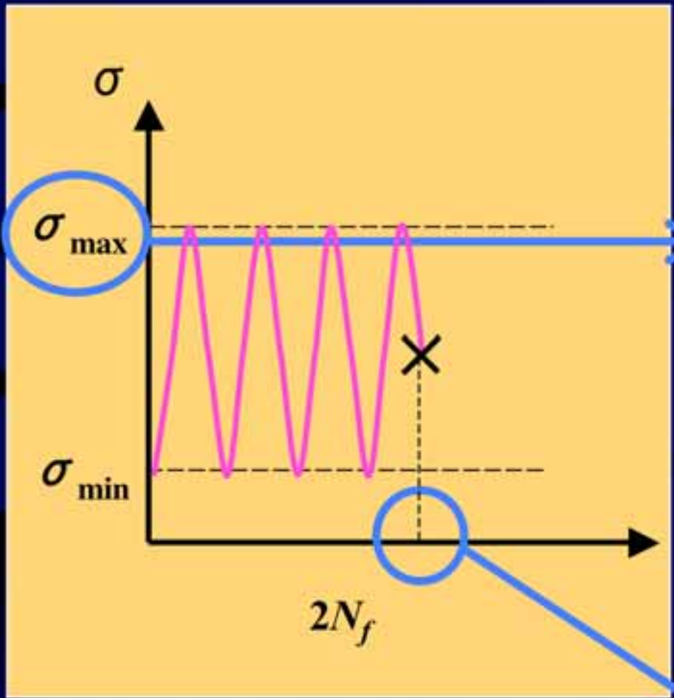

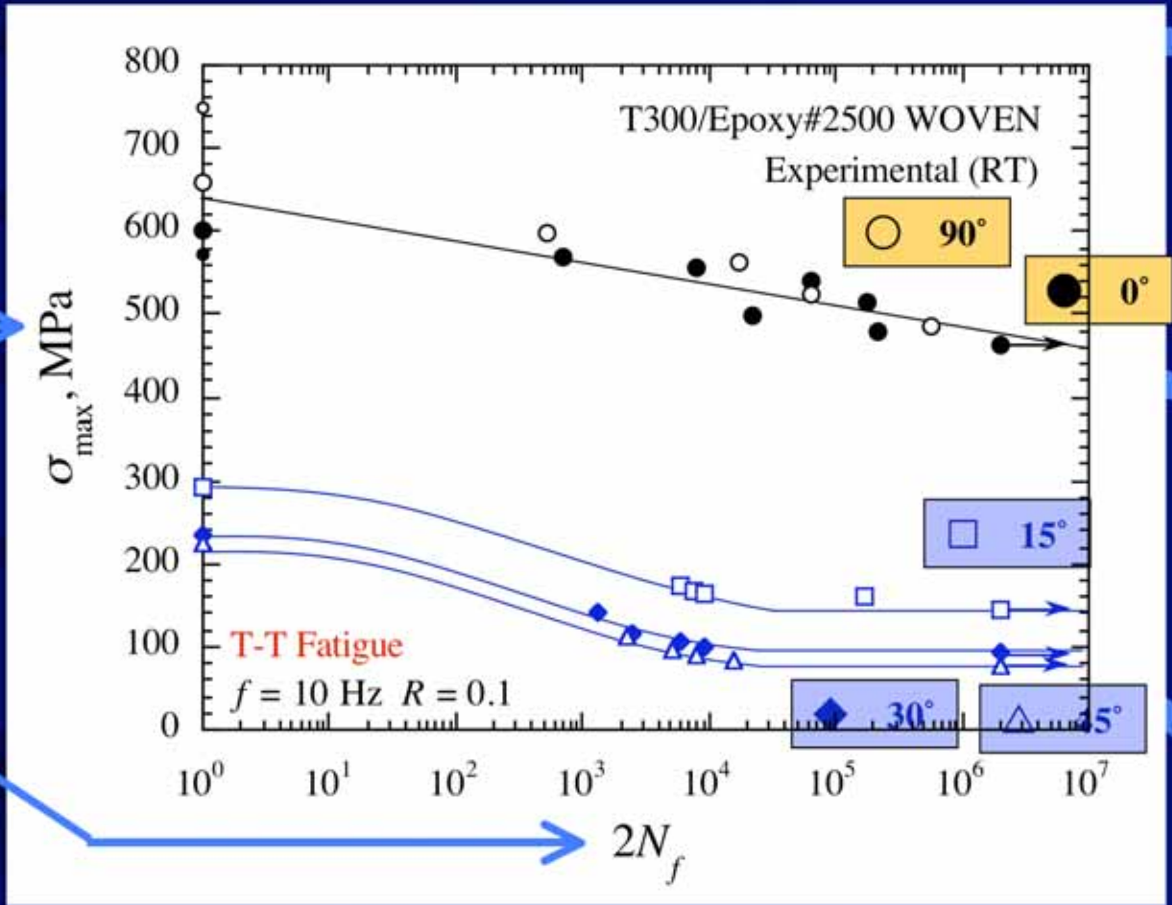

Temperature Dependence of Off-Axis S-N Curve

Comparisons between the S-N curves at RT and 100°C

$\theta = 15°$

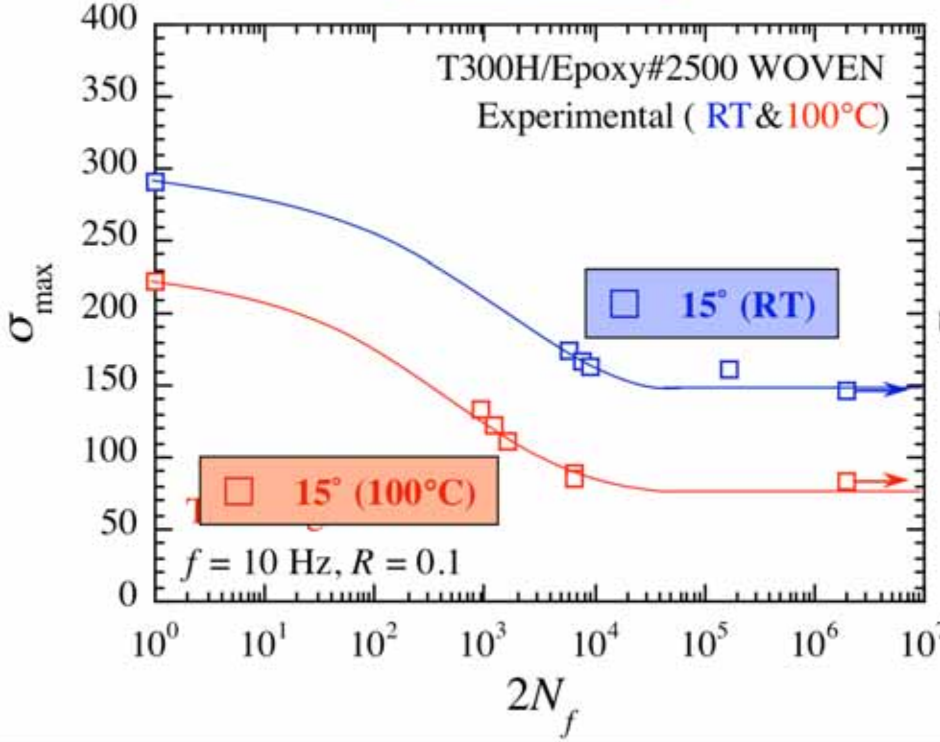

$\theta = 30°$

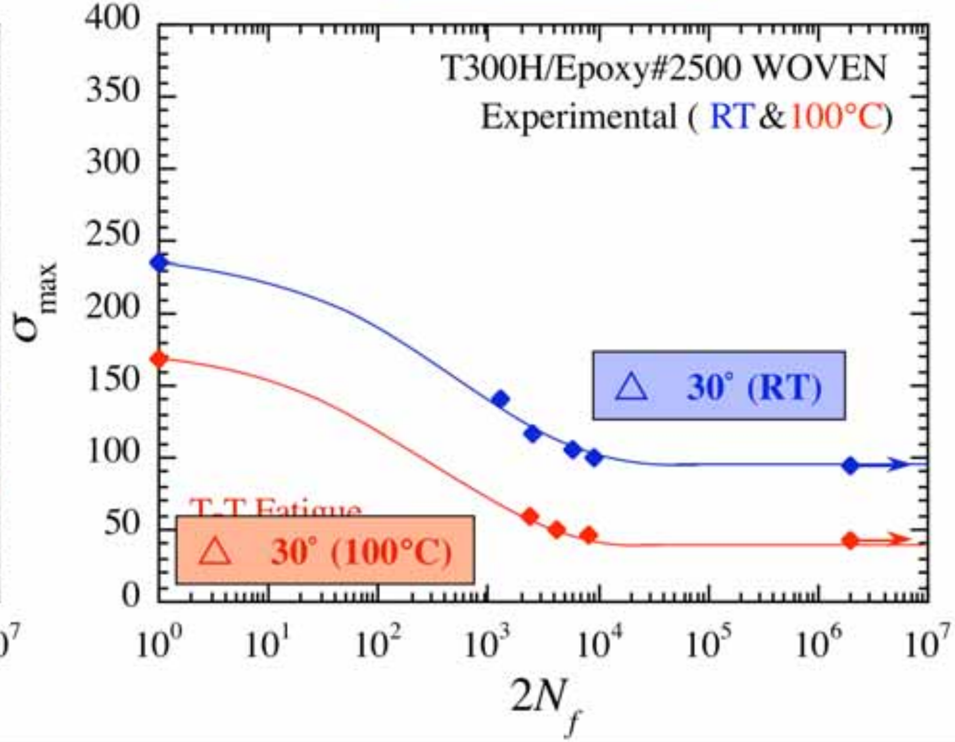

Fatigue Failure Morphology and Fatigue Limit

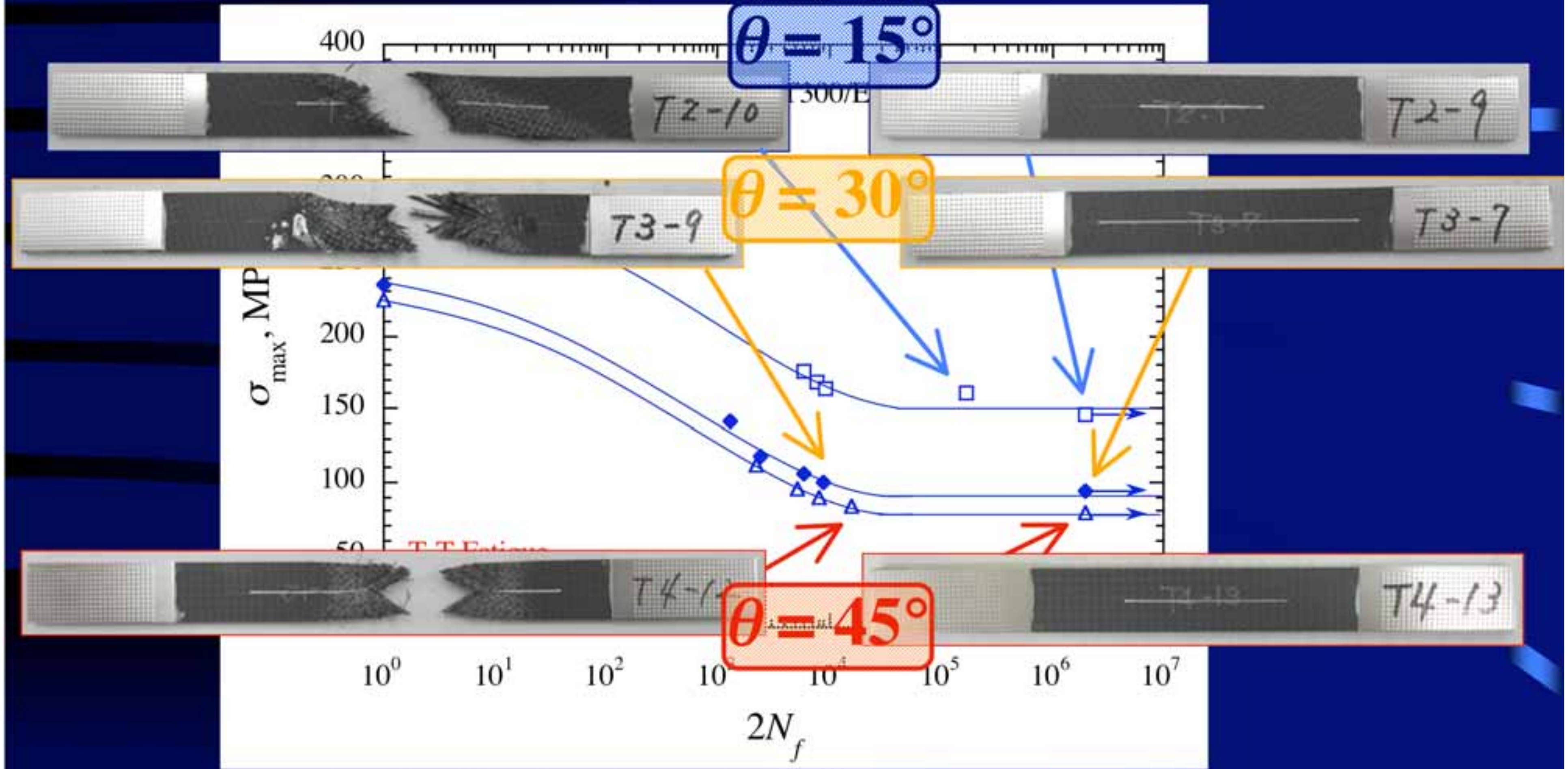

No major damage

Off-Axis S-N Curves for Woven CFRP Laminates

Assumption:

Orientation dependence of tensile strength

↓

Orientation dependence of fatigue strength

↓

Experimental strength ratio
$\sigma_{max}/\sigma_{B(exp)}$

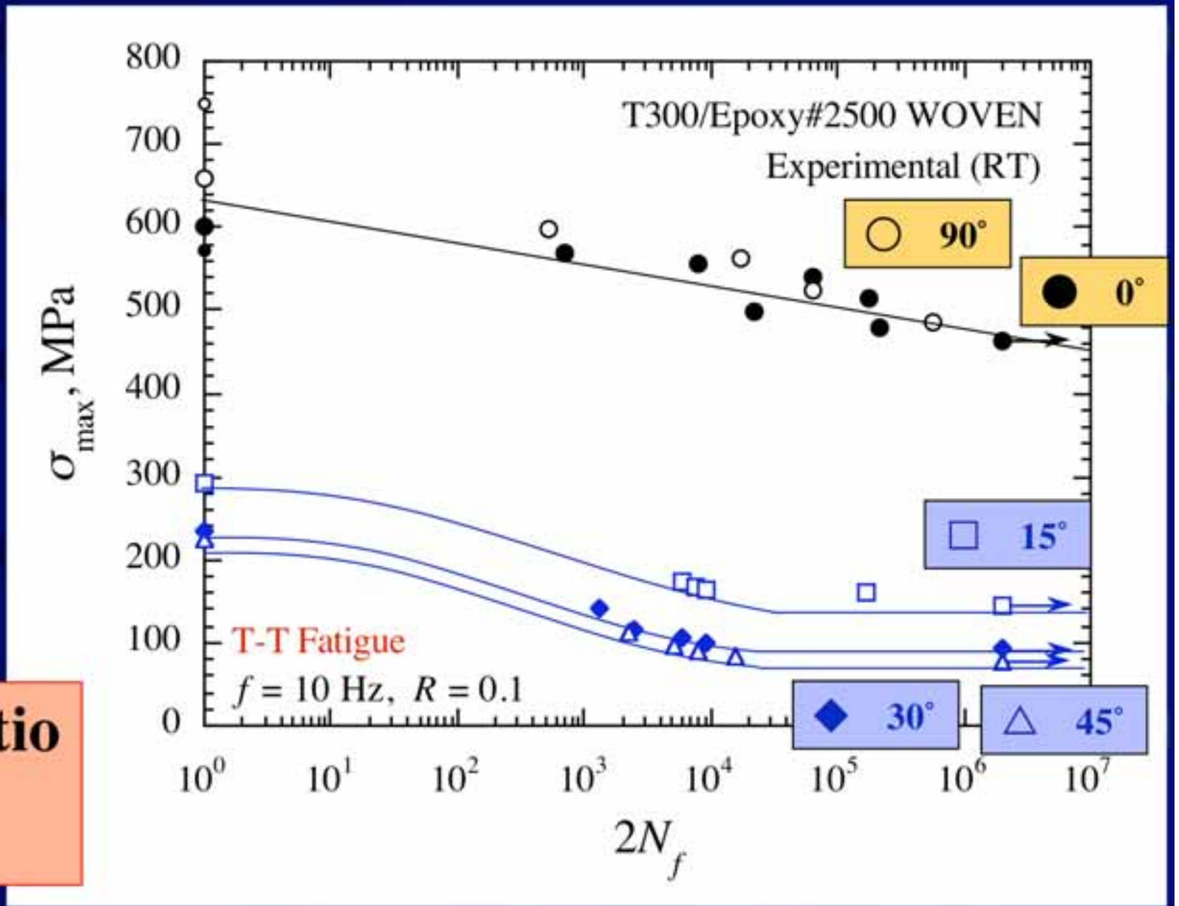

↑

What is an appropriate measure for modeling ?

Normalized S-N Relationships

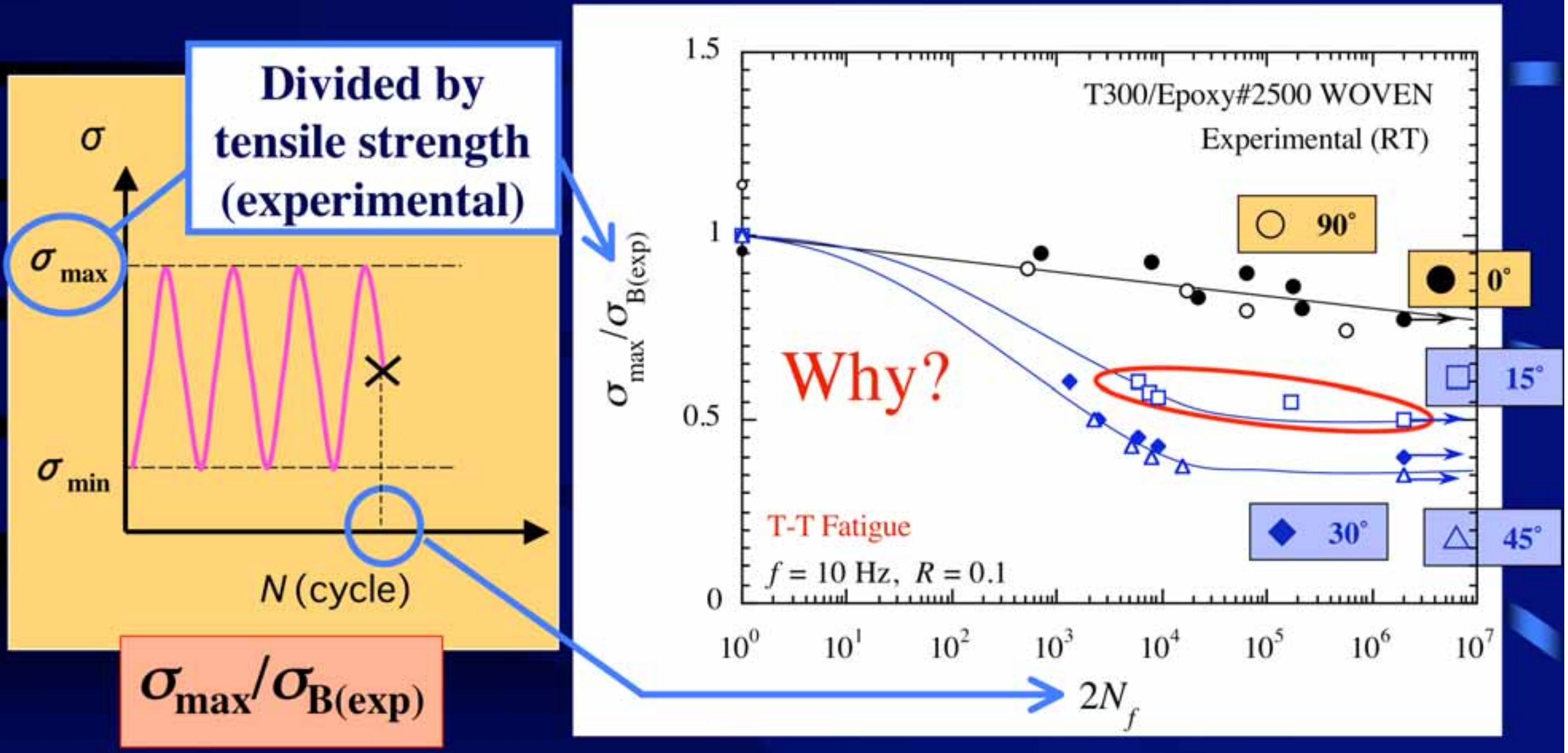

In this case, orientation dependence has not been removed completely using the experimental strength ratio !

Modified Tensile Strength

$$\sigma_x^f = \left[\frac{m^4 - m^2n^2}{\boxed{X^2}} + \frac{n^4}{\boxed{Y^2}} + \frac{m^2n^2}{\boxed{S^2}}\right]^{-1/2} \quad \begin{pmatrix} m = \cos\theta \\ n = \sin\theta \end{pmatrix}$$

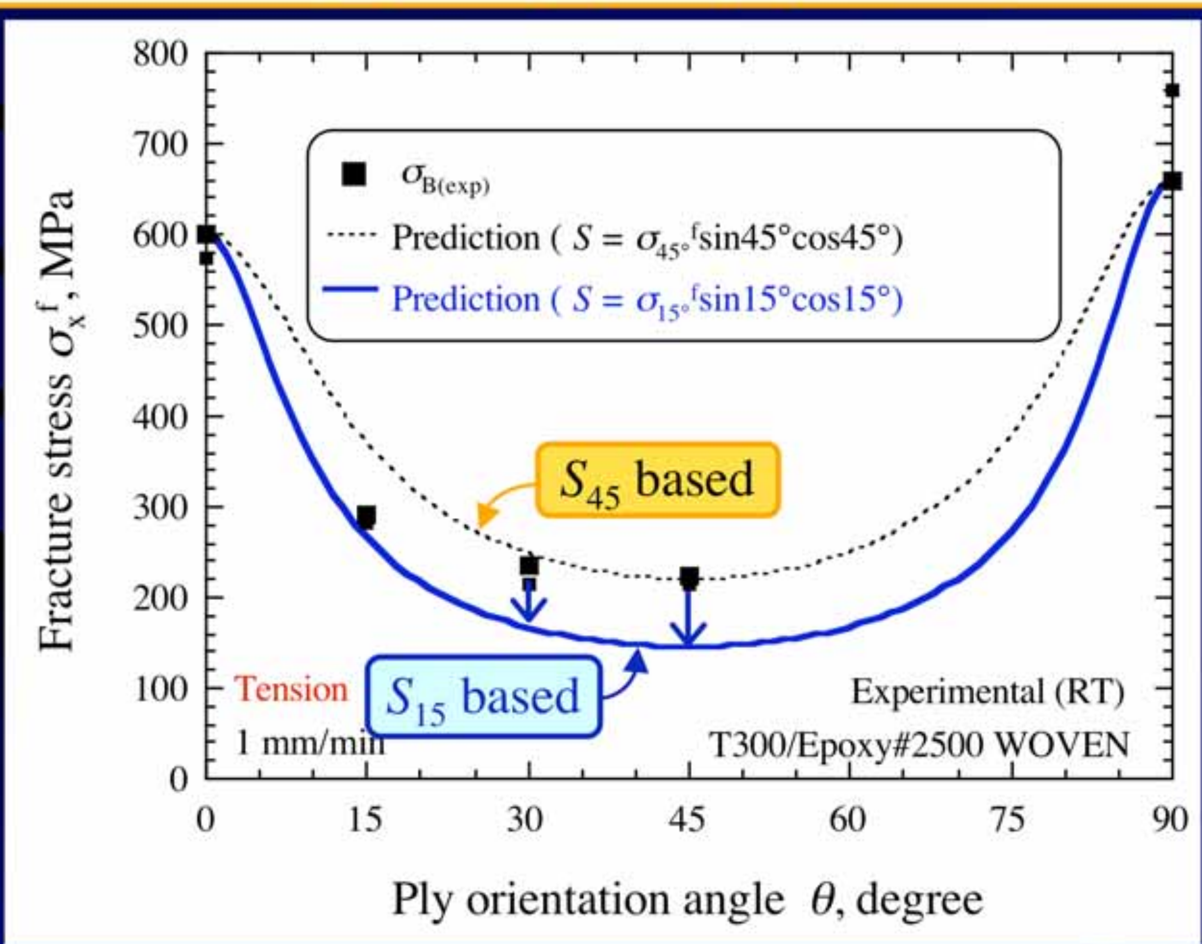

MPa

$\theta = 45°$ Basis

$X_{app} = \sigma_1^f = 599.5$

$Y_{app} = \sigma_2^f = 658.3$

$S_{app} = \tau_{12}^f = 112.0$

S_{45}

$\theta = 15°$ Basis

$X_{true} = \sigma_1^f = 599.5$

$Y_{true} = \sigma_2^f = 658.3$

$S_{true} = \tau_{12}^f = 72.9$

S_{15}

Theoretical Strength Ratio $\sigma^*_{max} = \sigma_{max} / \sigma_{B(pred)}$ v.s. $2N_f$

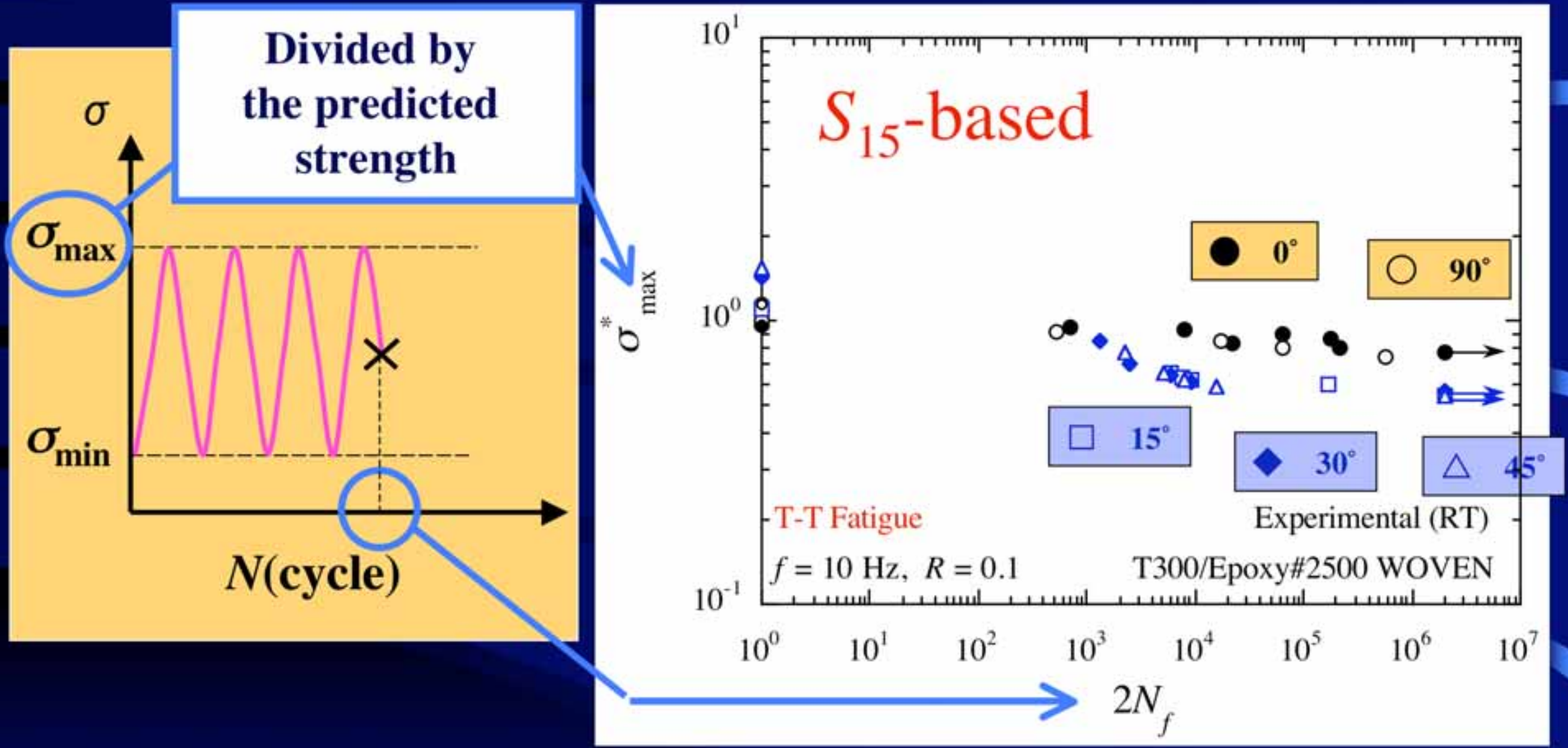

The fiber orientation dependence has been removed substantially by mean of S_{15}-based theoretical strength ratio.

A possibility of a lower strength for $\theta = 15°$ specimen

Fractured specimens

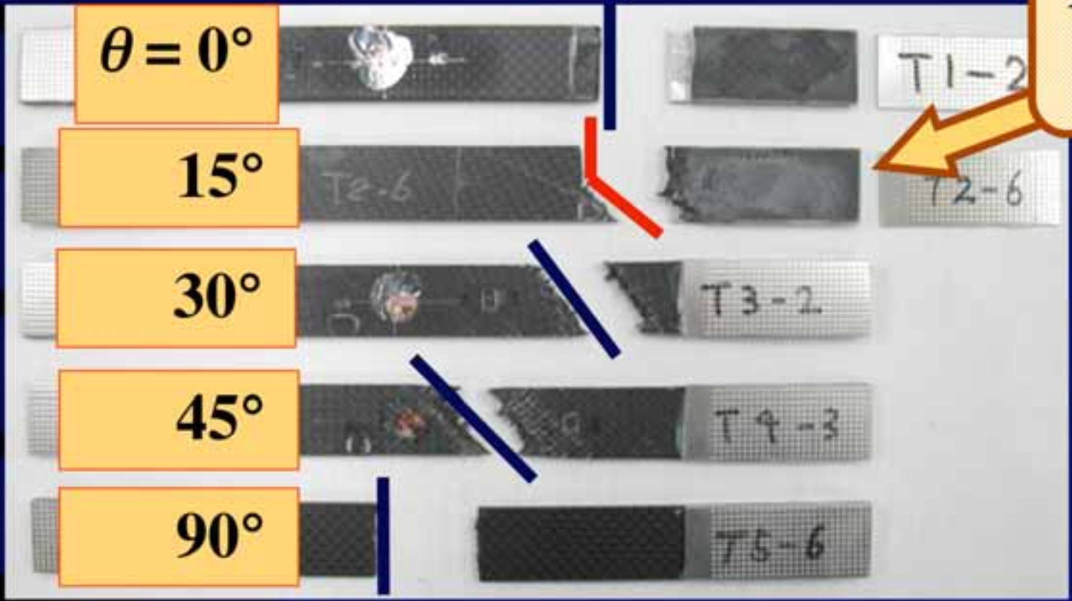

Fracture around tab not along fibers

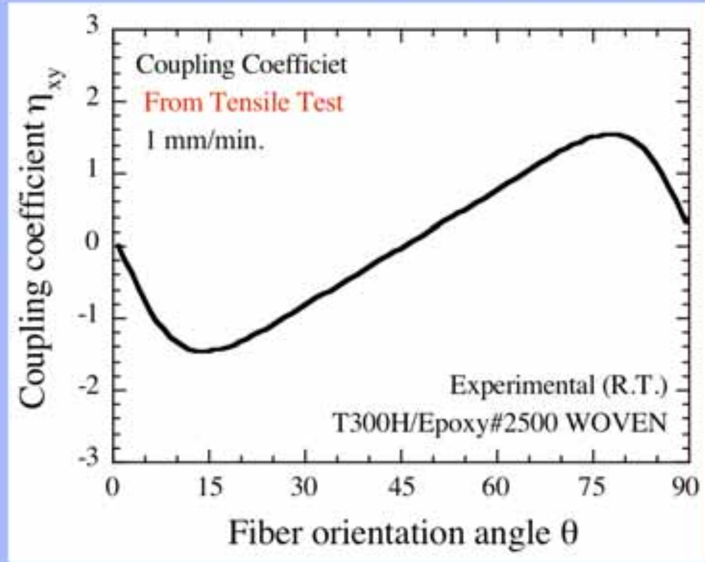

Prediction using FEM

High stress in the vicinity of tabs

Stress distribution of a specimen with tab AS4/3501-6(UD), $\theta = 10°$

(C.T. Sun, 1993)

Effects of End Constraint on the UTS for $\theta = 15°$

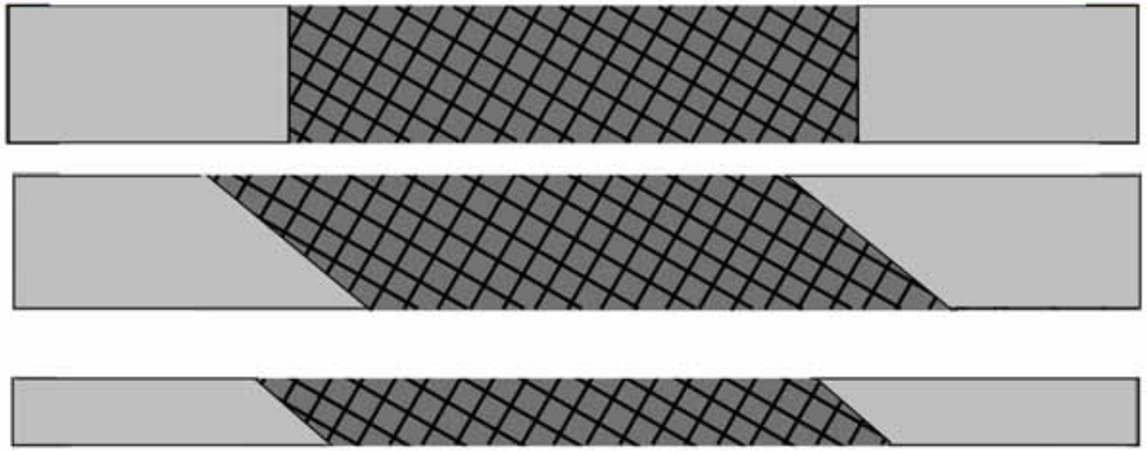

Rectangular tabs
(L/w = 5)

Oblique tabs
(L/w = 5)

(L/w = 10)

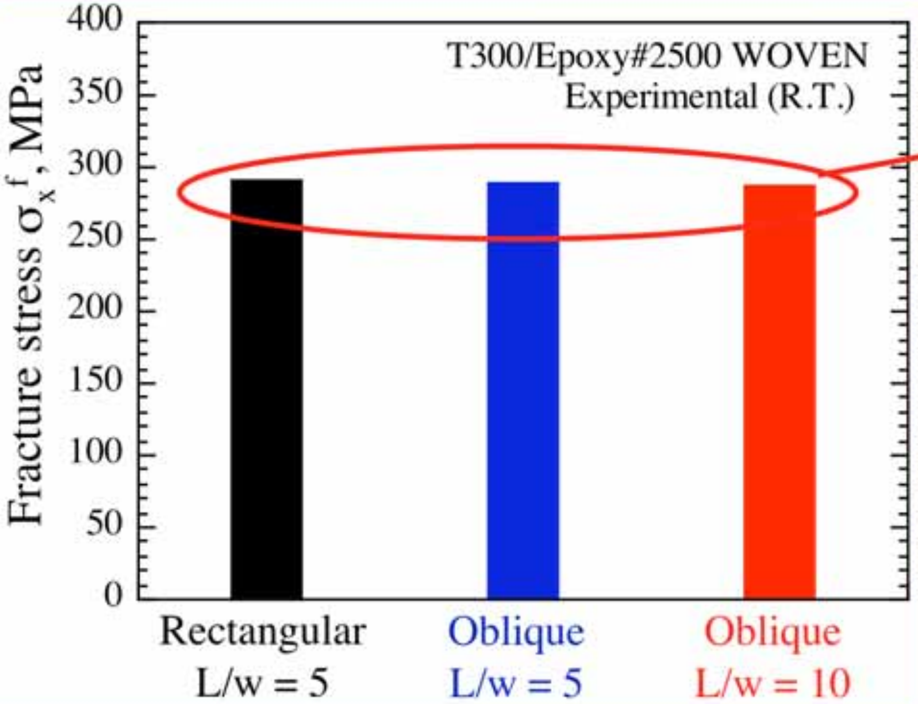

No significant difference

Not ascribed to $\theta = 15°$

Effect of Fiber Rotation

Static tension ($\theta = 45°$, 100°C)

θ	Off-axis angle at failure	
	RT	100°C
15°	15.0°	13.5°
30°	28.5°	22.3°
45°	34.2°	25.1°

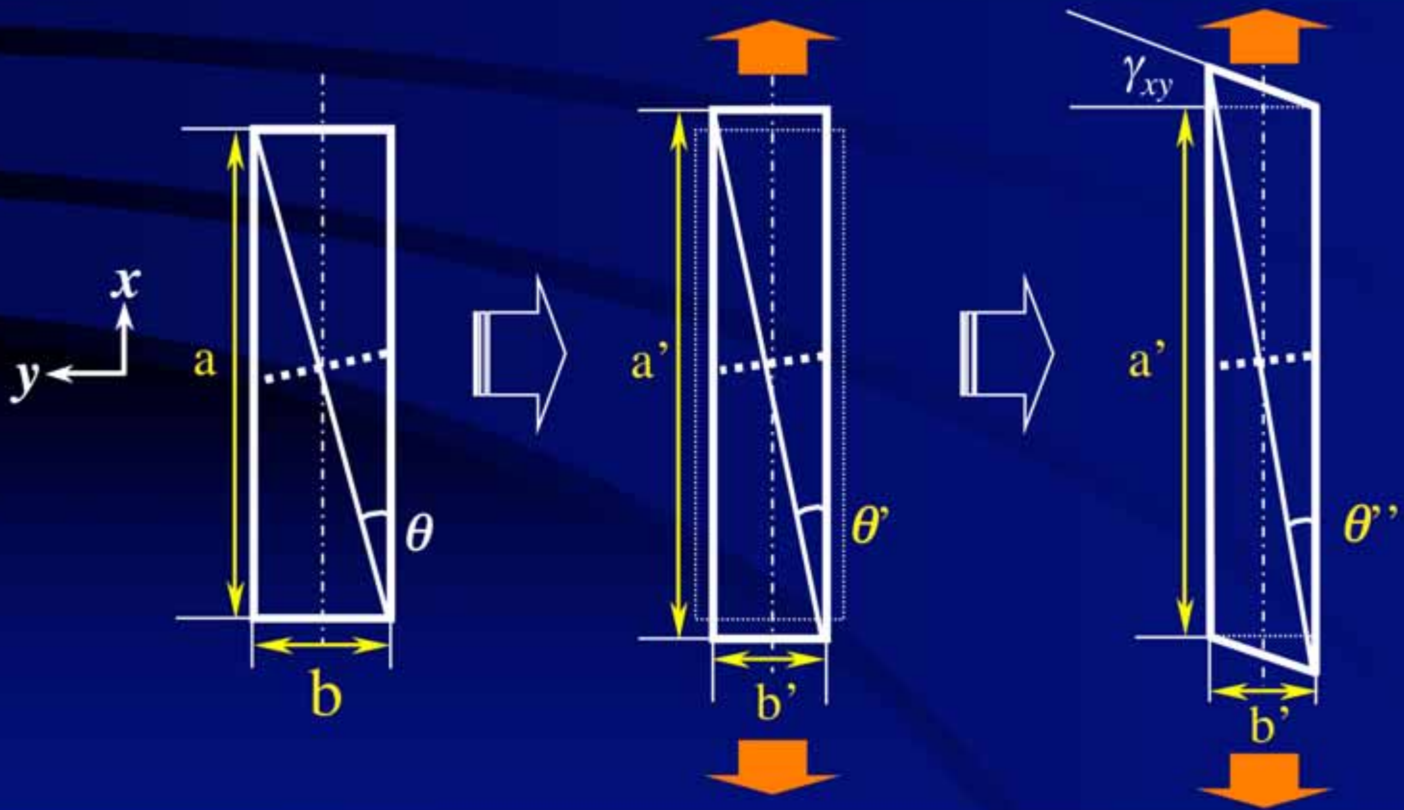

Modified Tensile Strength

$$\sigma_x^f = \left[\frac{m^4 - m^2 n^2}{\boxed{X^2}} + \frac{n^4}{\boxed{Y^2}} + \frac{m^2 n^2}{\boxed{S^2}} \right]^{-1/2} \qquad \begin{pmatrix} m = \cos\theta \\ n = \sin\theta \end{pmatrix}$$

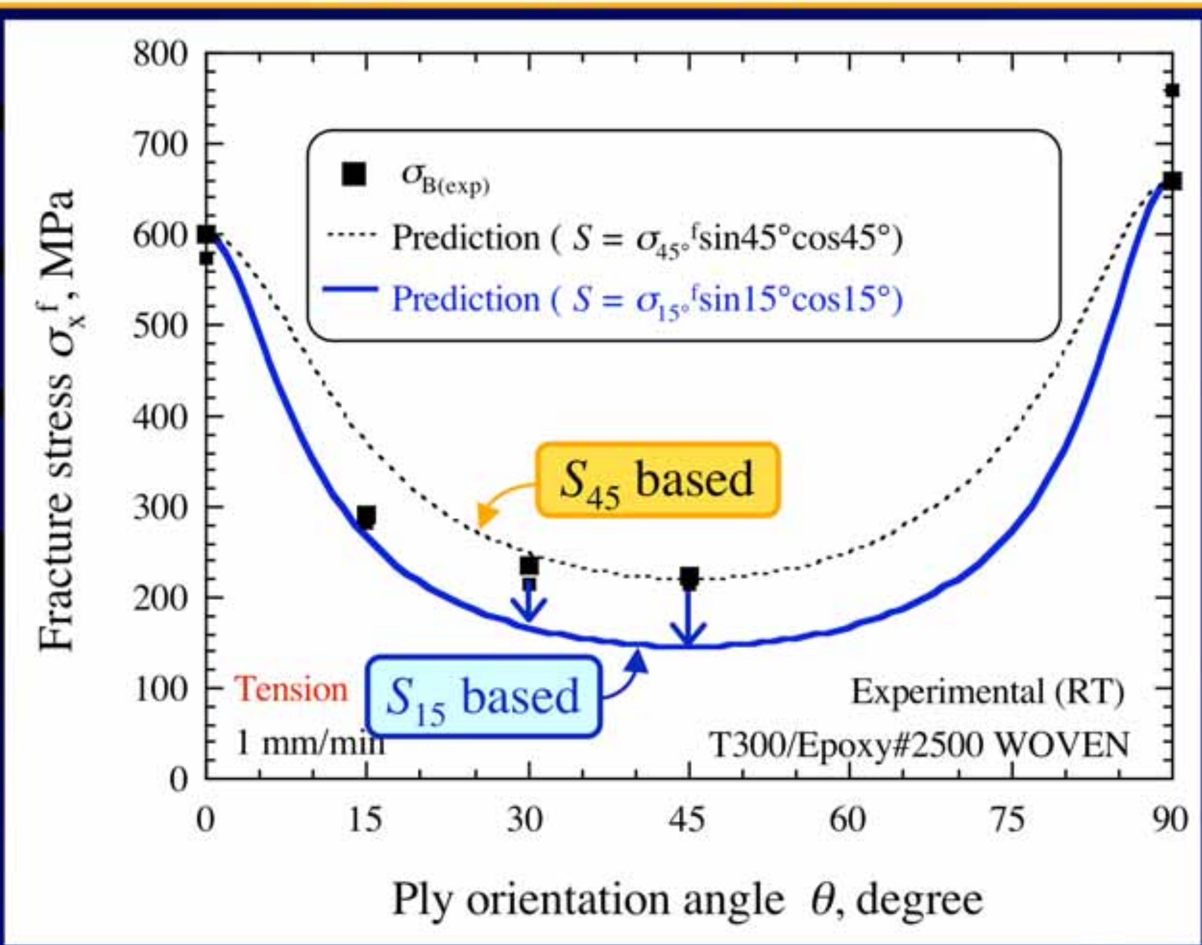

MPa

$\theta = 45°$ Basis

$X_{app} = \sigma_1^f = 599.5$

$Y_{app} = \sigma_2^f = 658.3$

$\boxed{S_{app} = \tau_{12}^f = 112.0}$

S_{45}

$\theta = 15°$ Basis

$X_{true} = \sigma_1^f = 599.5$

$Y_{true} = \sigma_2^f = 658.3$

$\boxed{S_{true} = \tau_{12}^f = 72.9}$

S_{15}

Theoretical Strength Ratio $\sigma^*_{max} = \sigma_{max} / \sigma_{B(pred)}$ v.s. $2N_f$

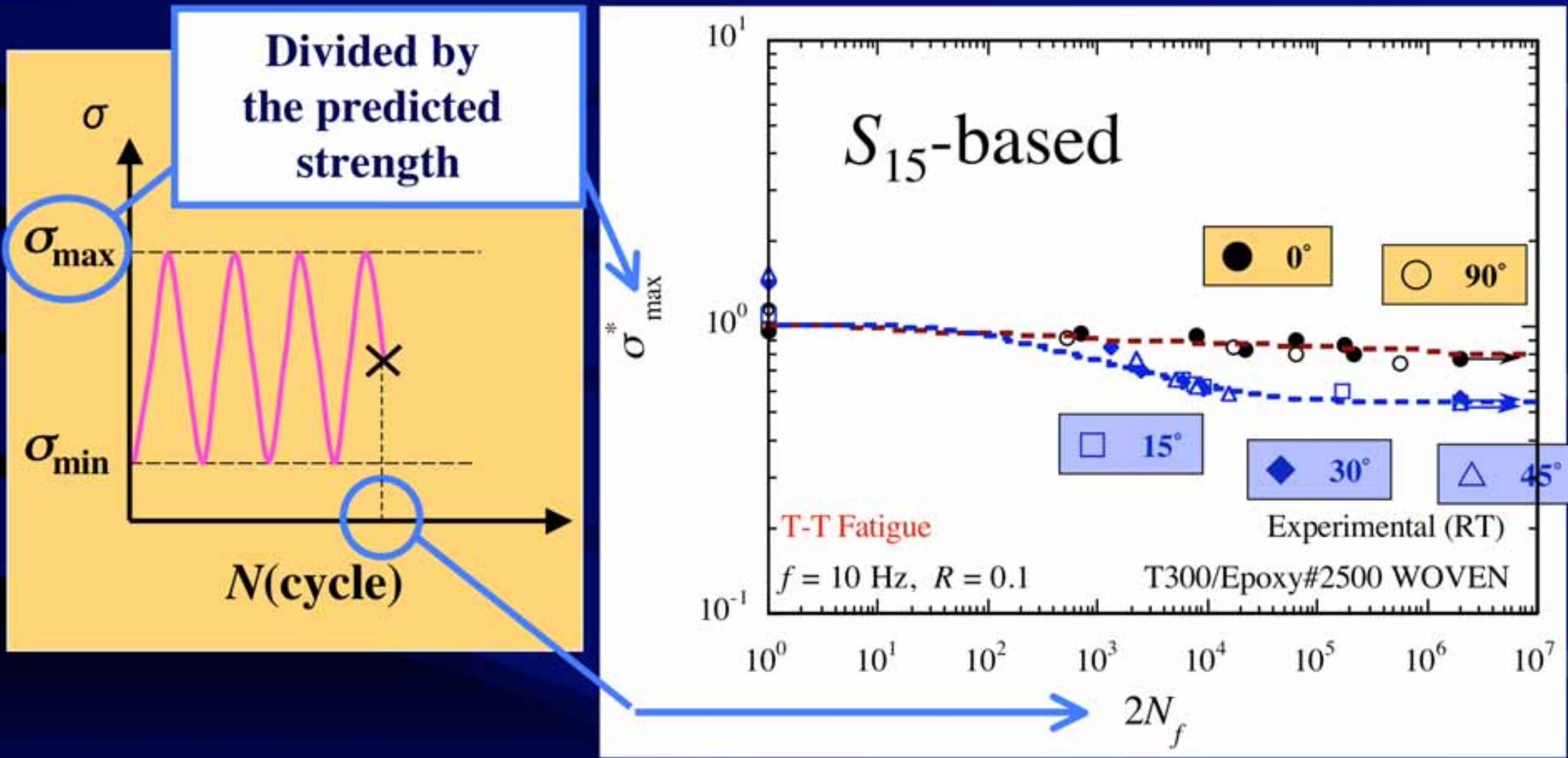

Master S-N relationships for the on-axis and off-axis fatigue behavior

Damage Mechanics Modeling of Composite Fatigue

- **Fatigue Damage Growth Law:**

$$\frac{d\omega}{dN} = K{\sigma^*_{\max}}^{n}\left(\frac{1}{1-\omega}\right)^{k}\frac{\langle\sigma^*_{\max}-\sigma^*_{L}\rangle^{b}}{\langle 1-\chi\sigma^*_{\max}\rangle^{a}}$$

- **Fatigue Life Equation:**

$$N_f = \frac{1}{(1+k)K{\sigma^*_{\max}}^{n}}\frac{\langle 1-\chi\sigma^*_{\max}\rangle^{a}}{\langle\sigma^*_{\max}-\sigma^*_{L}\rangle^{b}}$$

where

$$\sigma^* = \sqrt{\left(\frac{\sigma_{11}}{X}\right)^2-\frac{\sigma_{11}\sigma_{22}}{X^2}+\left(\frac{\sigma_{22}}{Y}\right)^2+\left(\frac{\tau_{12}}{S}\right)^2}$$

(Non-Dimensional Effective Stress)

On-Axis and Off-Axis Master Curves (RT)

Master S-N equation

$$2N_f = \frac{2}{(1+k)K\sigma^{*\,n}_{max}} \cdot \frac{\langle 1-\chi\sigma^{*}_{max}\rangle^{a}}{\langle \sigma^{*}_{max}-\sigma^{*}_{L}\rangle^{b}}$$

n: slope of $\sigma^{*}_{max} - 2N_f$

σ^{*}_{L} : Fatigue limit

$a, b, (1+k)K$: constants

On-axis constants

$n = 46.12, \quad \sigma^{*}_{L} = 0$

$a = 0, \quad b = 0$

$(1+k)K = 2$

Off-axis constants

$n = 6.31, \quad \sigma^{*}_{L} = 0.54$

$a = 0.6, \quad b = 0.7$

$(1+k)K = 0.015$

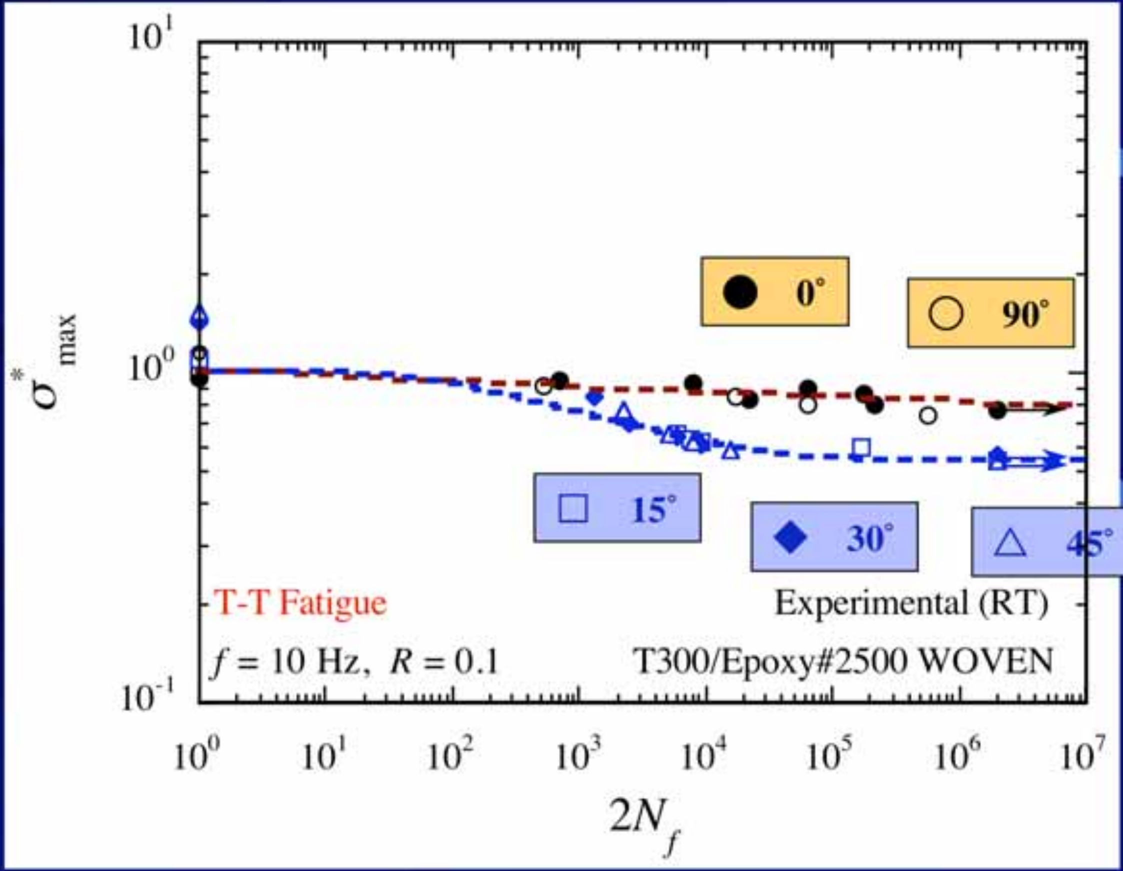

Predictions of S-N curves (RT)

$$\sigma^{*}_{\max} \cdot \sigma_{B(pred)} = \sigma_{\max}$$

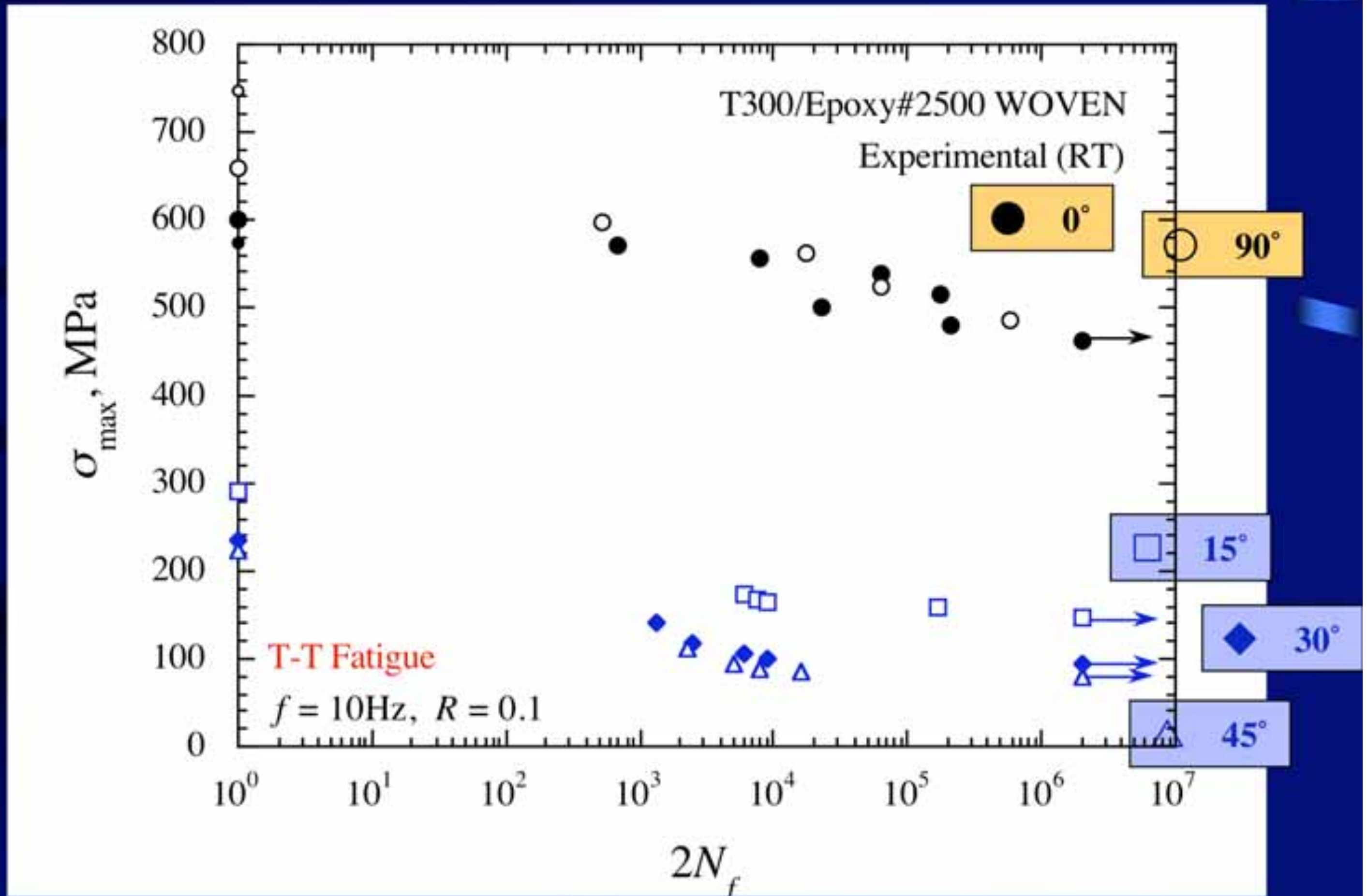

Predictions of S-N curves (RT)

$$\sigma^{*}_{\max} \cdot \sigma_{B(pred)} = \sigma_{\max}$$

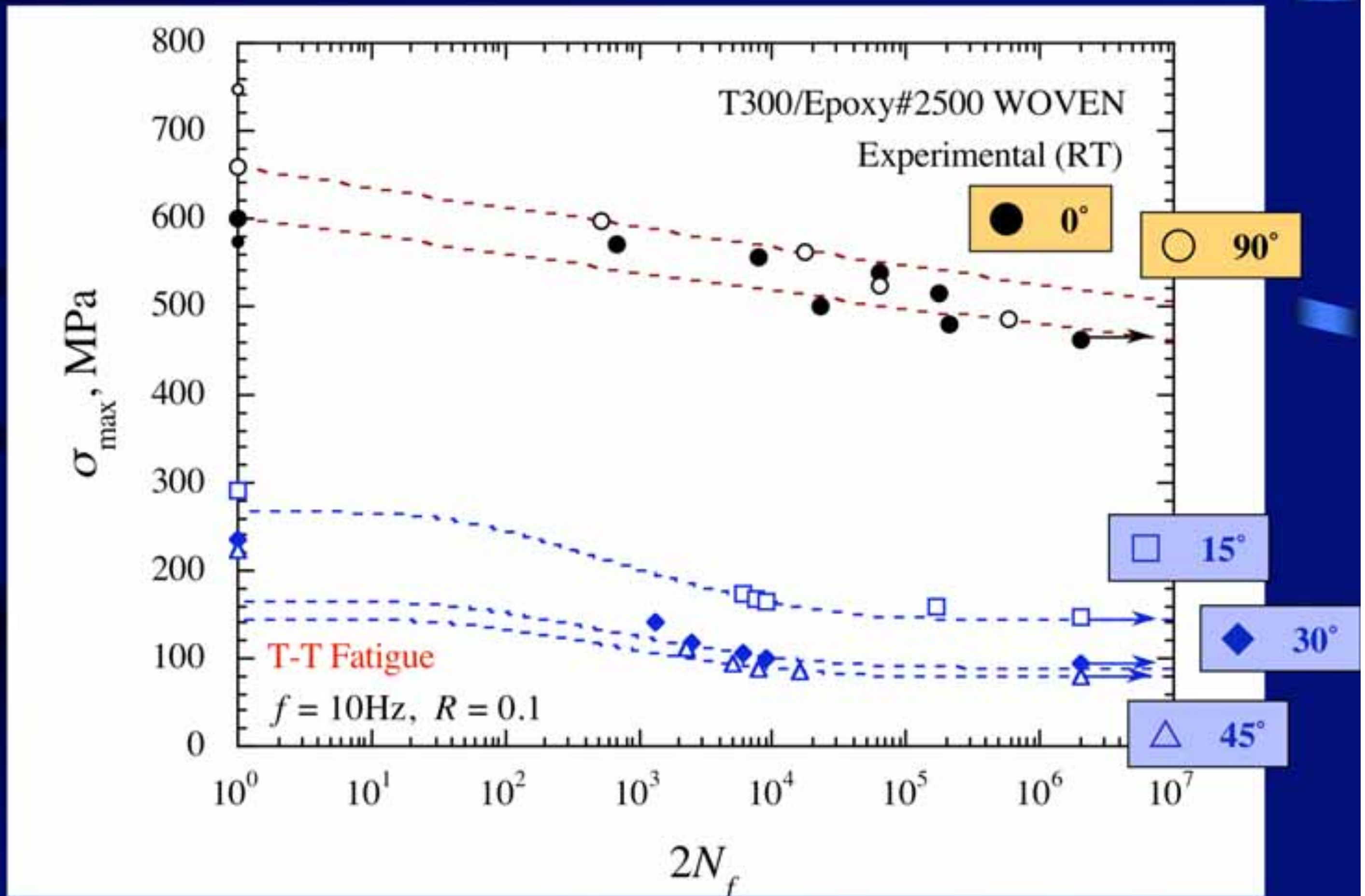

On- and Off-Axis Master Curves (100°C)

Master S-N equation

$$2N_f = \frac{2}{(1+k)K\sigma^{*\,n}_{max}} \cdot \frac{\langle 1-\chi\sigma^*_{max}\rangle^a}{\langle \sigma^*_{max}-\sigma^*_L\rangle^b}$$

n: slope of $\sigma^*_{max} - 2N_f$

σ^*_L : fatigue limit

$a, b, (1+k)K$: constants

On-axis constants

$n = 24.53, \quad \sigma^*_L = 0$

$a = 0, \quad b = 0$

$(1+k)K = 2$

Off-axis constants

$n = 4.49, \quad \sigma^*_L = 0.33$

$a = 0.9, \quad b = 0.2$

$(1+k)K = 0.02$

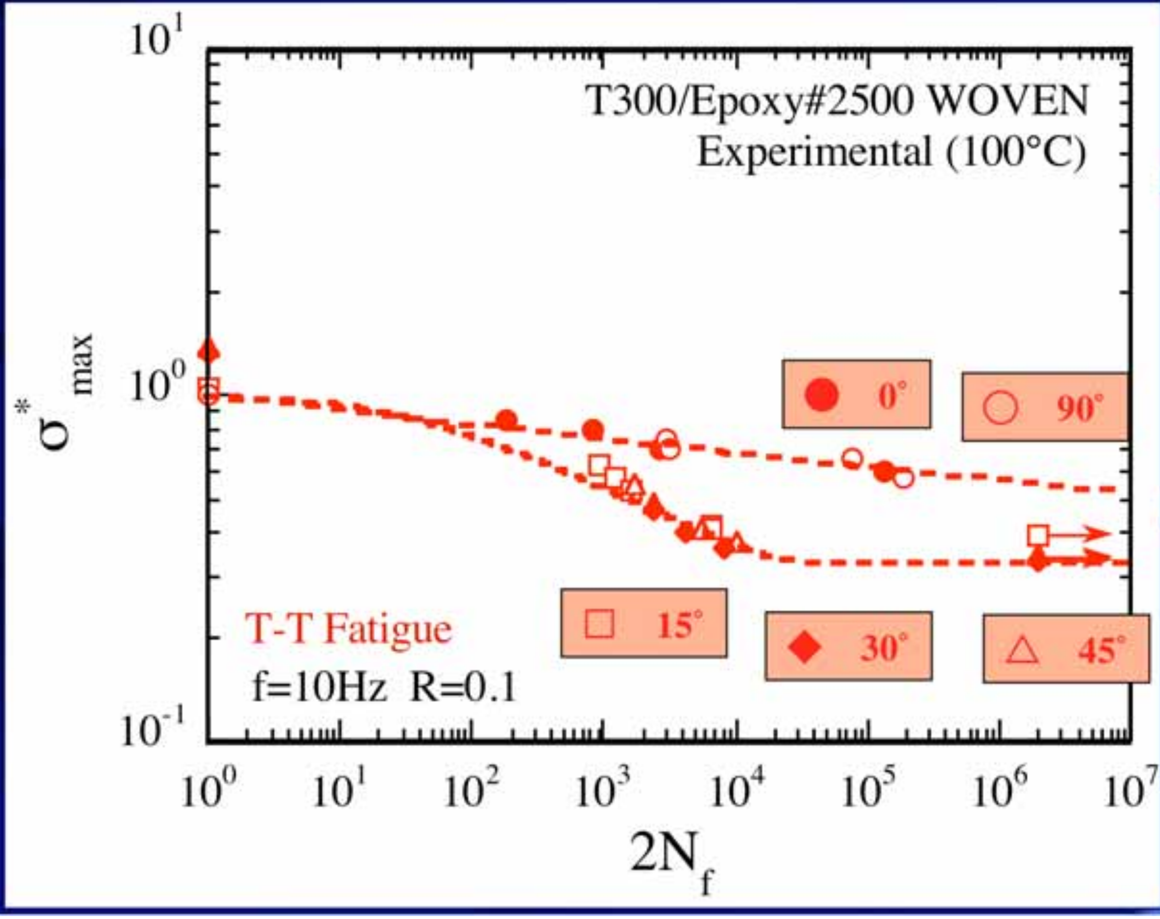

Predictions of S-N curves (100°C)

$$\sigma^{*}_{max} \cdot \sigma_{B(pred)} = \sigma_{max}$$

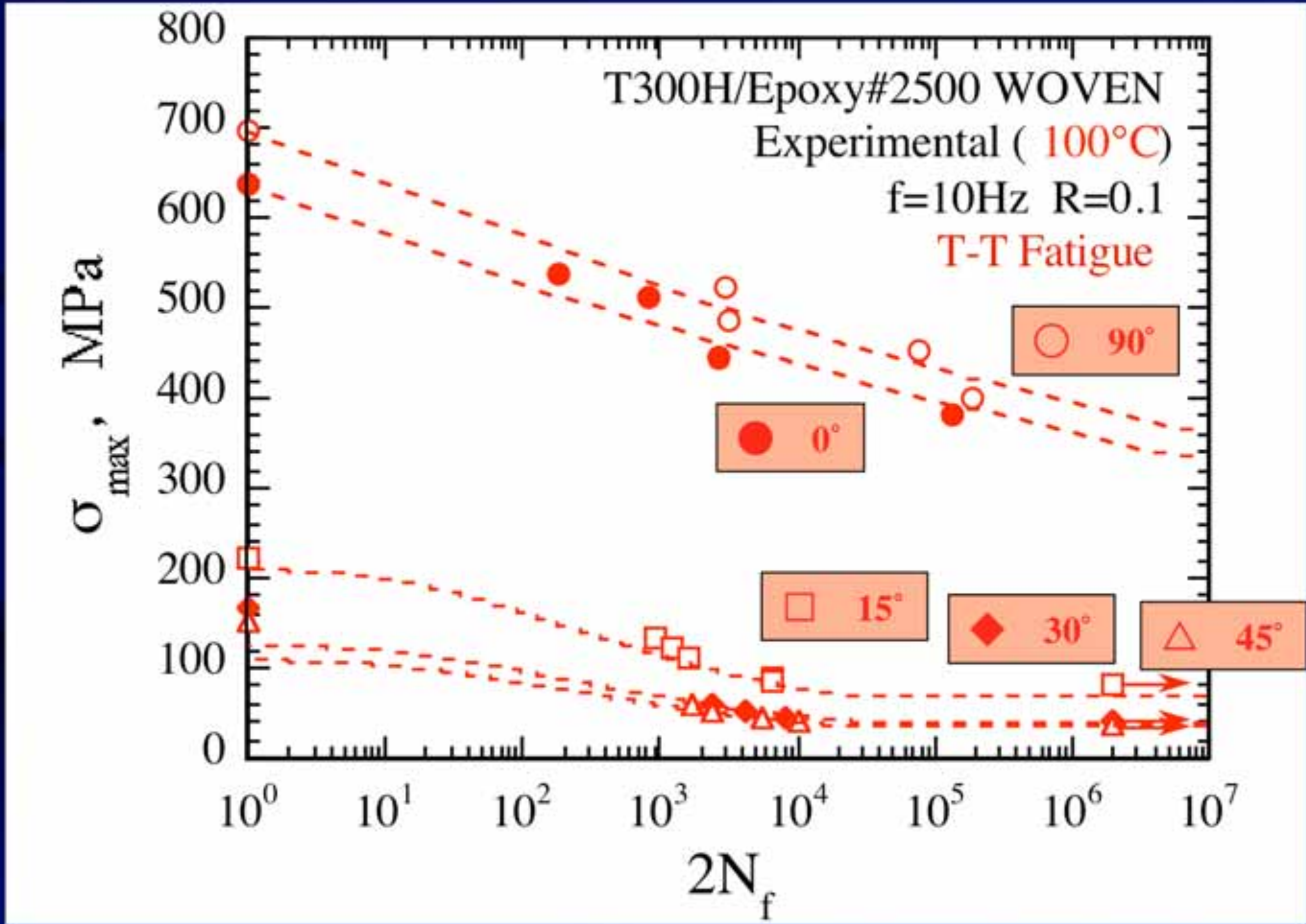

Self-Generated Heating During Fatigue Loading

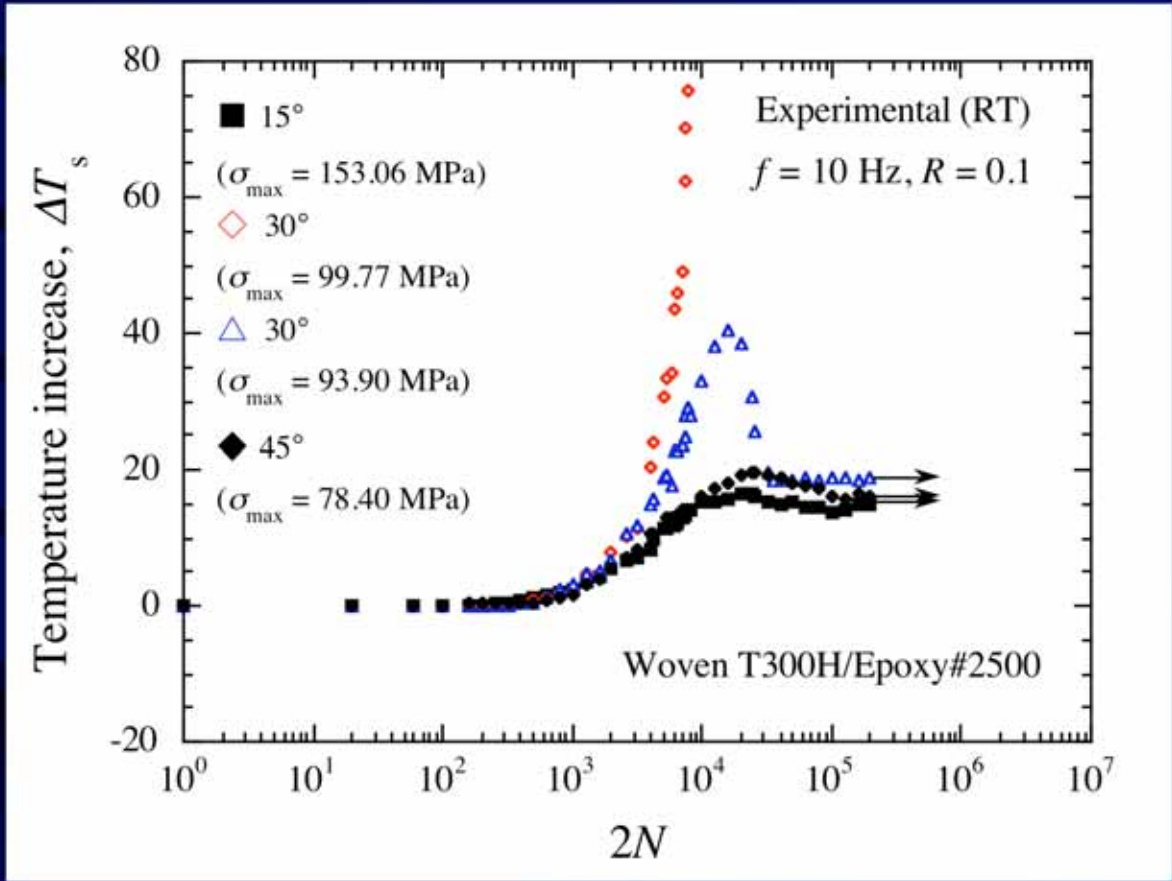

RT

(with an infrared radiation thermometer)

Frequency Dependence of Specimen Heating

RT

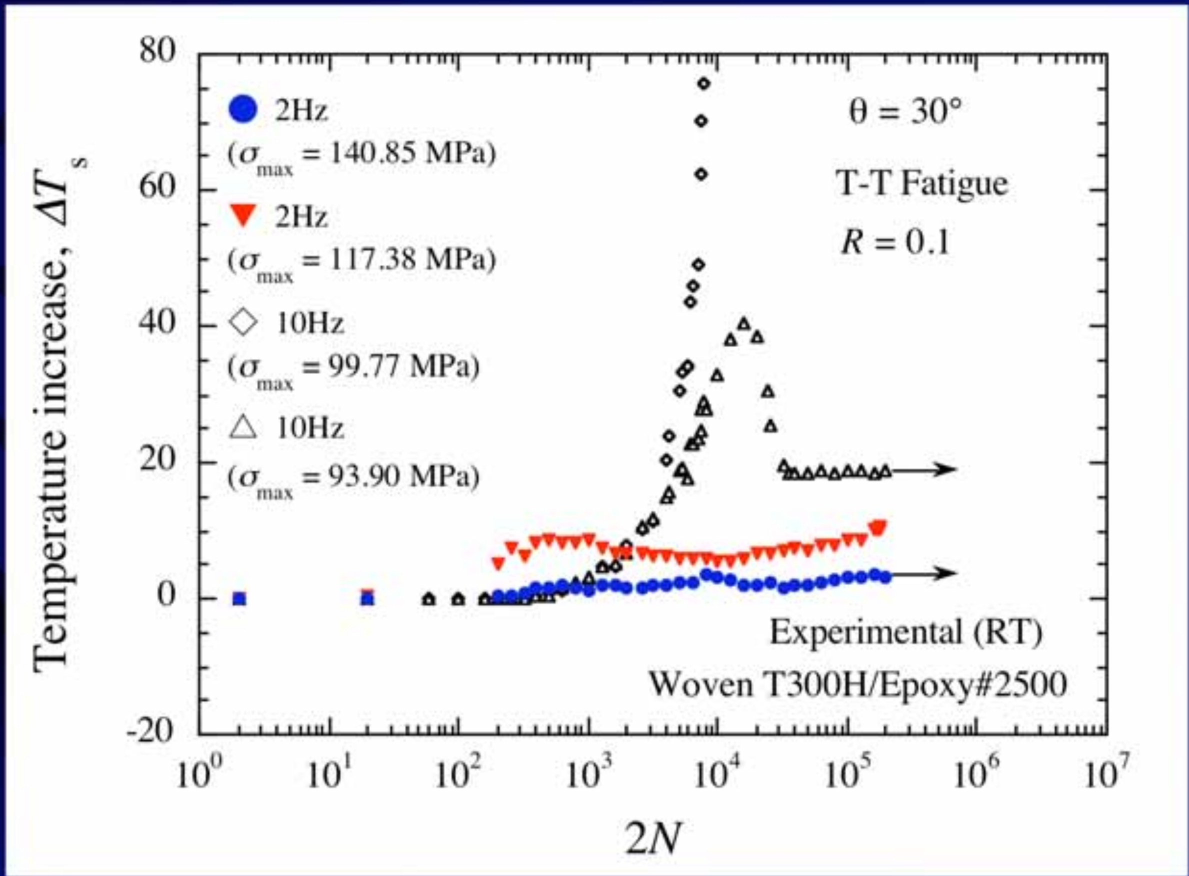

Off-Axis S-N Relationships at 2 and 10 Hz

RT

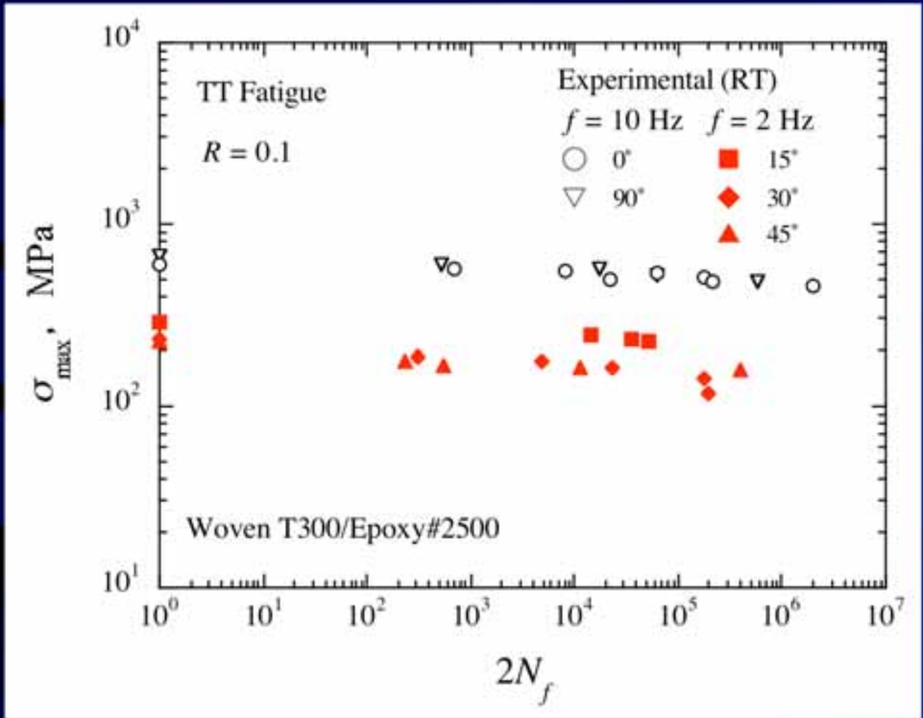

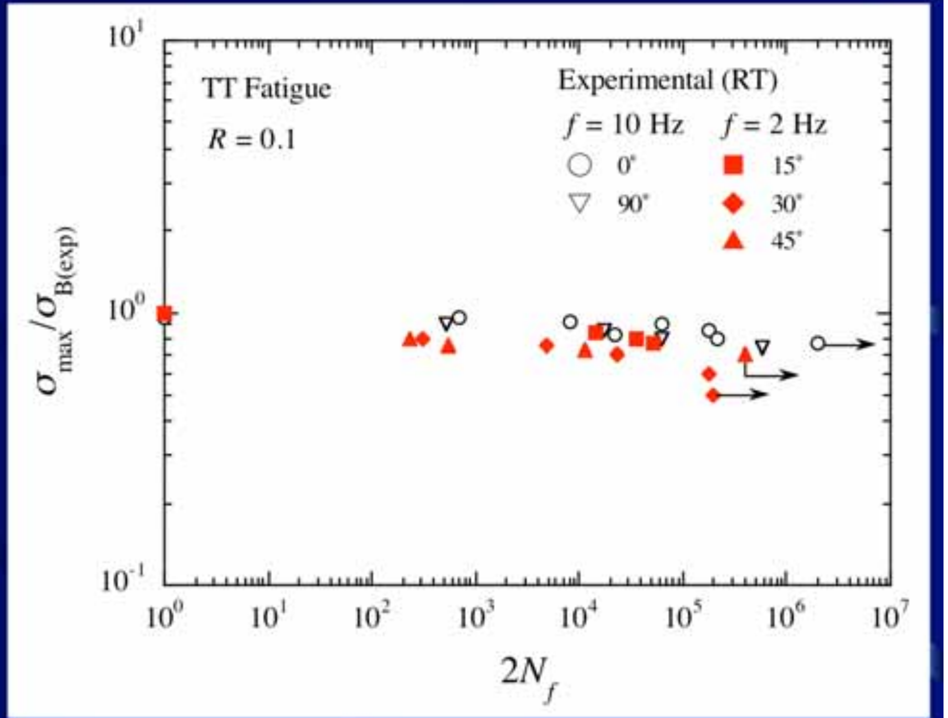

Intrinsic Frequency Dependence of Off-Axis Fatigue Behavior

100°C

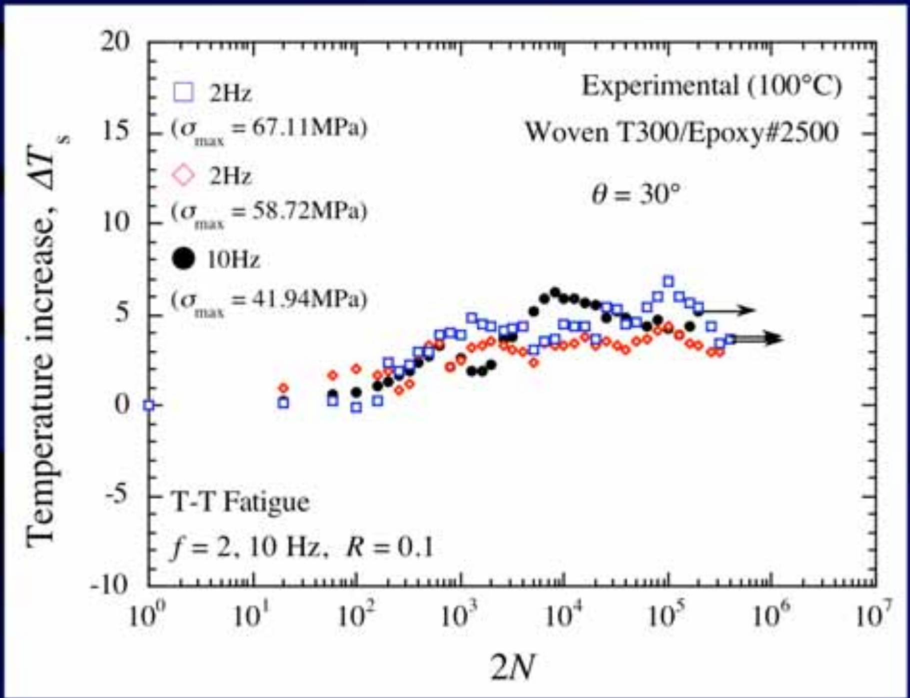

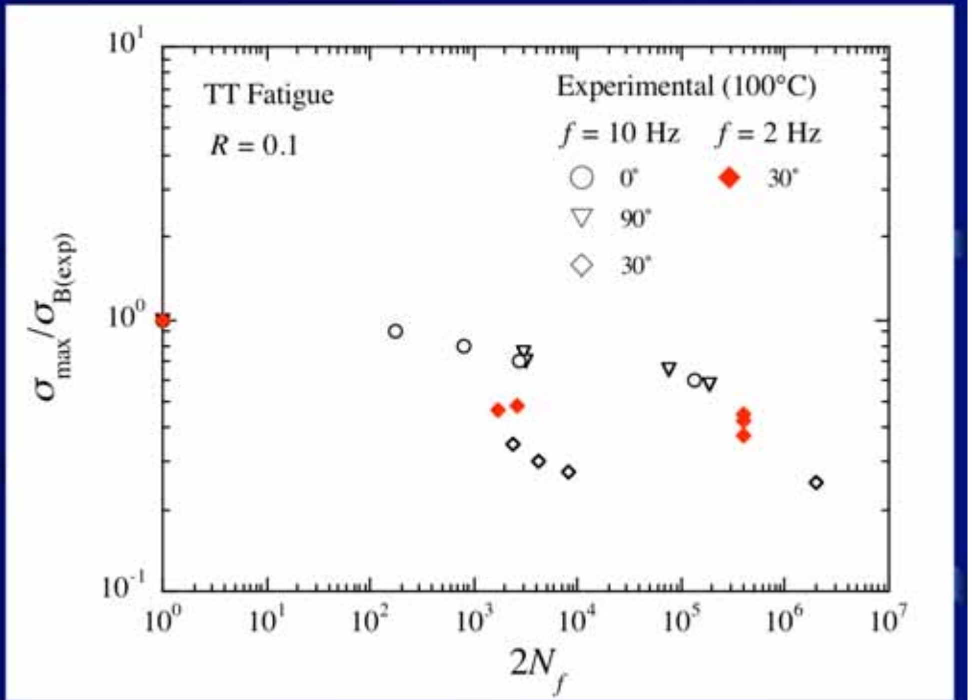

What we have seen

The S_{15}-based theoretical strength which takes a lower value for the fiber orientations $\theta = 30$ and 45° has worked to compensate for the effect of strength reduction due to self-generated heating during fatigue loading.

Appropriate determination of the principal shear strength is crucial to a successful application of a strength-based fatigue failure criterion.

Conclusions

The off-axis tensile fatigue behavior of plain weave carbon fabric laminates at room temperature and 100°C were examined.

Applicability of a phenomenological fatigue model was evaluated by comparing with the experimental results at a fixed frequency of 10 Hz.

Fatigue behavior

- The off-axis S-N relationship is characterized by its S-shape, regardless of the fiber orientations and test temperatures.
- The off-axis fatigue strength is much lower than the on-axis fatigue strength and it becomes smaller with increasing off-axis angle from 15 to 45°, regardless of the test temperatures.

Conclusions

Continued

- The theoretical strength ratio defined appropriately becomes a useful parameter to cope with the fiber orientation dependence of the off-axis fatigue behavior of the woven carbon fabric laminate.
- The S-N data normalized using the S_{15}-based theoretical strength separate well into two groups associated with the on-axis and off-axis directions, regardless of the test temperatures.
  The normalized off-axis S-N data eventually fall on a single S-N relationship for each of the test temperatures.
- The S-shape of the off-axis S-N relationships at 10 Hz is caused mainly by the reduction in strength due to temperature rise of specimen during fatigue loading and partly by a rate-dependent property of the material.

Conclusions

Continued

Fatigue model

- The potential usefulness of a phenomenological fatigue model has been demonstrated.
- The fatigue model that assumes two master S-N curves for on-axis and off-axis fatigue loading succeeds in adequately describing the fatigue behavior of the plain weave carbon/epoxy composite laminate with a frequency of 10 Hz at room temperature and 100°C.
- A single master S-N curve version of the fatigue model is likely to be successfully applied to the room-temperature fatigue behavior at a lower frequency (≤ 2 Hz) of fatigue loading.

Thank you for your kind attention !